



PERGAMON

Available online at www.sciencedirect.com

SCIENCE @ DIRECT®

Polyhedron 22 (2003) 433–439



POLYHEDRON

www.elsevier.com/locate/poly

Bimetallic sandwiches assembled with chelated Cu/Zn cations and manganese dicyanamide polymeric ladders

Zhe-Ming Wang^a, Bai-Wang Sun^a, Jun Luo^a, Song Gao^a, Chun-Sheng Liao^a,
Chun-Hua Yan^{a,*}, Yong Li^b

^a State Key Laboratory of Rare Earth Materials Chemistry and Applications, PKU-HKU Joint Laboratory on Rare Earth Materials and Bioinorganic Chemistry, Peking University–Nonius B.V. Demo Lab for X-Ray Diffraction, Peking University, Beijing 100871, China

^b Department of Chemistry, Tsinghua University, Beijing 100084, China

Received 14 August 2002; accepted 4 November 2002

Abstract

Two isomorphous bimetallic polymeric transition metal dicyanamides [Cu(OAc)(bpy)₂][Mn(dca)₃(H₂O)] (1) and [Zn(OAc)(bpy)₂][Mn(dca)₃(H₂O)] (2) (bpy = 2,2'-bipyridine, dca = dicyanamide) have been synthesized and characterized. Each consists of Mn–dca ladder chain anions and chelated cations of the other metal, Cu or Zn. The novel ladder-like [Mn(dca)₃(H₂O)][−]_n chains build a pseudo-(4,4) sheet through hydrogen bonds between the chains. The [M(OAc)(bpy)₂]⁺ (M = Cu, Zn) cations form a layer through weak C–H···O hydrogen bonds and π–π interactions. These oppositely charged sheets construct a sandwich structure by conventional O–H···O hydrogen bonds and weak C–H···C/N/O interactions. The Mn²⁺ ions are octahedrally coordinated in both compounds, while Cu²⁺ and Zn²⁺ ions have distorted octahedral environments. Magnetic investigation shows that the coupling interaction between Mn²⁺ centers of the ladder Mn–dca chains is weak antiferromagnetic.

© 2002 Elsevier Science Ltd. All rights reserved.

Keywords: Bimetallic coordination polymers; Dicyanamide; Crystal structures; Magnetic properties; Sandwich; Template

1. Introduction

Coordination polymers of dicyanamide (N(CN)₂[−], dca) have attracted intense interest due to their diversity in both topologies and magnetic properties [1,2]. The ligand, dca, is a remarkably versatile building block for the construction of supramolecular architectures since it may act as a uni-, bi- and tri- dentate ligand [3]. Many extended homometallic coordination polymers are known, for example, 3-D for M^{II}[N(CN)₂]₂, (M = Cu, Co, Ni, Mn) [4], 2-D for Zn[N(CN)₂]₂ [5], and 1-D three-leg ladder for Zn₃(Ac)₄(4,4'-bpy)₃[N(CN)₂]₂ [6]. However, only a few heterometallic dca compounds [7–9] have been reported, including [M(bpy)₃][M'(dca)₃]₂ (M = Fe, M' = Mn/Fe or M = Ni, M' = Mn) [7]. The

latter consists of [M'(bpy)₃]²⁺ cations and unusual (6, 3) sheets of [M(dca)₃][−], and the cations are embedded in the hexagonal windows of the sheet. In our previous studies, several novel bimetallic networks were obtained by employing unsaturated chelate cations, which display sheet, threefold interpenetrating diamond-like net [8] and unusually deeply interdigitated thick bimetallic layer structures [9]. Other organic cations, such as PPh₄⁺ and AsPh₄⁺, were also used to construct unusual assemblies with 1D to 3D anionic dca coordination polymers of [M(dca)₄][−], [M₂(dca)₆(H₂O)]^{2−} and [M(dca)₃][−] [10]. All these results reveal that the composite architectures as well as the anionic dicyanamide polymers are cation-templated, and it is worthy to carry out further investigations. Here we report the structural and magnetic characterization of two isomorphous bimetallic polymers, [Cu(OAc)(bpy)₂][Mn(dca)₃(H₂O)] (1) and [Zn(OAc)(bpy)₂][Mn(dca)₃(H₂O)] (2)

* Corresponding author. Tel./fax: +86-10-6275-4179.

E-mail address: chyan@chem.pku.edu.cn (C.-H. Yan).

(bpy = 2,2'-bipyridine), each composed of Mn–dca chains and chelated cations of the other metal, Cu or Zn.

2. Experimental

2.1. Materials and measurements

All reagents were commercial grade and used as received. Elemental analyses for C, H, N and metals were carried out by an Elementar Vario EL instrument and ICP method, respectively. IR spectra were recorded on a Nicolet Magna-IR 750 spectrometer for neat samples in the range of 4000–650 cm^{-1} . EPR spectra of polycrystalline samples were recorded with a Bruker ER200D-SRC spectrometer at X-band frequency ($\nu = 9775$ MHz) at room temperature. Magnetic measurements were performed on an Oxford MagLab 2000 system in the temperature range of 2–300 K under 1 T field. Diamagnetic corrections, -354×10^{-6} and $-358 \times 10^{-6} \text{ cm}^3 \text{ mol}^{-1}$ for **1** and **2**, respectively, were estimated using Pascal's constants [11].

2.2. Preparation of complexes

2.2.1. $[\text{Cu}(\text{OAc})(\text{bpy})_2][\text{Mn}(\text{dca})_3(\text{H}_2\text{O})]$ (**1**)

A 5 ml EtOH solution of bpy (94 mg, 0.60 mmol) and $\text{Cu}(\text{OAc})_2 \cdot \text{H}_2\text{O}$ (60 mg, 0.30 mmol) was mixed with 5 ml aqueous-EtOH solution of Na(dca) (53 mg, 0.60 mmol) and $\text{Mn}(\text{OAc})_2 \cdot 4\text{H}_2\text{O}$ (74 mg, 0.30 mmol). The deep blue filtrate was left for slow evaporation. Blue–green crystals of block shape were obtained after 2 weeks, which (yield 19%) were collected and washed with EtOH (*Anal.* Found: C, 47.73; H, 3.08; N, 24.97; Cu, 8.50; Mn, 7.43. $\text{C}_{28}\text{H}_{21}\text{CuMnN}_{13}\text{O}_3$ requires: C, 47.63; H, 3.00; N, 25.79; Cu, 9.00; Mn, 7.78%; ν/cm^{-1} (4000–650): (OH) 3250w br; (ArH) ~ 3000 w br; (CN) 2288s; (CO) 1600m, 1569m and 1553m; (bpy) 1493m, 1474m, 1445s, 1414m and 768s; $\lambda_{\text{max}}/\text{nm}$: 700 and 280.

2.2.2. $[\text{Zn}(\text{OAc})(\text{bpy})_2][\text{Mn}(\text{dca})_3(\text{H}_2\text{O})]$ (**2**)

The above procedure was repeated by employing $\text{Zn}(\text{OAc})_2 \cdot 2\text{H}_2\text{O}$ (66 mg, 0.30 mmol) in place of $\text{Cu}(\text{OAc})_2 \cdot \text{H}_2\text{O}$, producing light yellow block-shaped crystals of **2** in 12% yield (*Anal.* Found: C, 47.44; H,

Table 1
Crystallographic data for compounds **1** and **2**

Complex no.	1	2
Empirical formula	$\text{C}_{28}\text{H}_{21}\text{CuMnN}_{13}\text{O}_3$	$\text{C}_{28}\text{H}_{21}\text{MnN}_{13}\text{O}_3\text{Zn}$
Formula weight	706.06	707.89
Space group	$P\bar{1}$	$P\bar{1}$
<i>a</i> (Å)	8.8593(2)	8.8382(2)
<i>b</i> (Å)	11.5231(4)	11.4766(4)
<i>c</i> (Å)	15.3168(6)	15.4501(5)
α (°)	77.2230(13)	77.0489(12)
β (°)	88.207(2)	88.4121(16)
γ (°)	86.684(2)	86.8440(17)
<i>V</i> (Å ³)	1522.09(9)	1524.77(8)
<i>Z</i>	2	2
<i>D</i> _{calc} (g cm ⁻³)	1.541	1.542
<i>F</i> (000)	716	718
Crystal size (mm ³)	0.40 × 0.22 × 0.09	0.35 × 0.30 × 0.20
θ Range (°)	3.45–27.88	3.45–32.03
Limiting indices	$-11 \leq h \leq 11, -15 \leq k \leq 15, -20 \leq l \leq 20$	$-13 \leq h \leq 13, -17 \leq k \leq 17, -23 \leq l \leq 23$
Total reflections	27414	29895
Unique reflections	7208	10361
<i>R</i> _{int} ^a	0.0513	0.0372
obs. ($I \geq 2\sigma(I)$)	5441	7215
μ (Mo K α) (mm ⁻¹)	1.168	1.255
Trans. factor	0.905 and 0.829	0.789 and 0.745
<i>R</i> ₁ ^b , <i>R</i> _w ^c (for obs.)	0.0392, 0.0881	0.0408, 0.0867
<i>R</i> ₁ ^b , <i>R</i> _w ^c (all data)	0.0622, 0.0973	0.0722, 0.0974
Max. shift/sigma	0.002	0.001
Goodness-of-fit ^d	1.048	1.018
$\Delta\rho$ ^e (e Å ⁻³)	0.525, -0.508	0.536, -0.575

^a $R_{\text{int}} = \Sigma |F_o^2 - F_o^2(\text{mean})| / \Sigma [F_o^2]$.

^b $R_1 = \Sigma ||F_o| - |F_c|| / \Sigma |F_o|$.

^c $R_w = \{ \Sigma [w(F_o^2 - F_c^2)^2] / \Sigma [w(F_o^2)^2] \}^{1/2}$, $w = 1 / [\sigma^2(F_o^2) + (aP)^2 + bP]$, $P = [2F_c^2 + \text{Max}(F_o^2, 0)] / 3$.

^d Goodness-of-fit = $\{ \Sigma [w(F_o^2 - F_c^2)^2] / (n-p) \}^{1/2}$.

^e Maximum and minimum peaks in the final difference Fourier syntheses.

3.09; N, 25.07; Mn, 8.07; Zn, 8.92. $C_{28}H_{21}MnN_{13}O_3Zn$ requires: C, 47.51; H, 2.99; N, 25.72; Mn, 7.76; Zn, 9.24%; ν/cm^{-1} (4000–650): (OH) 3263w br; (ArH) \sim 3000w br; (CN) 2288s, 2233s and 2163vs; (CO) 1598s, 1577s, 1568s and 1547sh; (bpy) 1491m, 1474m, 1441s, 1420sh, 767s and 737m; λ_{max}/nm : 280.

2.3. X-ray crystallography

Table 1 gives the details of crystallographic data for **1** and **2**. Intensity data of **1** and **2** were collected at 293 K

Table 2
Selected bond lengths (Å) and angles (°) for **1** and **2**

	Complex 1 , M = Cu	Complex 2 , M = Zn
<i>Bond lengths</i>		
M(1)–O(1)	2.013(2)	2.120(1)
M(1)–O(2)	2.672(2)	2.347(2)
M(1)–N(1)	2.006(2)	2.121(2)
M(1)–N(2)	2.173(2)	2.107(2)
M(1)–N(3)	1.993(2)	2.137(2)
M(1)–N(4)	2.046(2)	2.115(2)
Mn(1)–O(3)	2.166(2)	2.179(2)
Mn(1)–N(5)	2.174(2)	2.175(2)
Mn(1)–N(8)	2.238(2)	2.237(2)
Mn(1)–N(11)	2.246(2)	2.236(2)
Mn(1)–N(10A)	2.226(2)	2.227(2)
Mn(1)–N(13B)	2.236(2)	2.223(2)
<i>Bond angles</i>		
O(1)–M(1)–O(2)	53.98(6)	58.29(5)
O(1)–M(1)–N(1)	89.95(7)	92.86(6)
O(1)–M(1)–N(2)	100.47(7)	99.33(5)
O(1)–M(1)–N(3)	90.05(7)	88.59(6)
O(1)–M(1)–N(4)	153.06(7)	152.99(6)
O(2)–M(1)–N(1)	91.95(7)	91.67(5)
O(2)–M(1)–N(2)	153.12(6)	155.23(5)
O(2)–M(1)–N(3)	87.26(7)	89.60(6)
O(2)–M(1)–N(4)	100.16(6)	98.35(5)
N(1)–M(1)–N(2)	78.56(7)	78.07(6)
N(1)–M(1)–N(3)	179.03(8)	178.43(6)
N(1)–M(1)–N(4)	99.31(7)	101.86(6)
N(2)–M(1)–N(3)	102.40(7)	101.12(6)
N(2)–M(1)–N(4)	106.13(7)	105.76(6)
N(3)–M(1)–N(4)	80.29(8)	77.03(6)
O(3)–Mn(1)–N(5)	88.39(9)	89.57(7)
O(3)–Mn(1)–N(8)	172.85(8)	172.25(7)
O(3)–Mn(1)–N(11)	87.02(8)	86.83(7)
O(3)–Mn(1)–N(10A)	88.33(9)	87.64(7)
O(3)–Mn(1)–N(13B)	92.75(8)	91.85(7)
N(5)–Mn(1)–N(8)	93.63(9)	93.85(7)
N(5)–Mn(1)–N(11)	91.42(9)	90.64(7)
N(5)–Mn(1)–N(10A)	174.64(8)	175.67(7)
N(5)–Mn(1)–N(13B)	86.16(8)	86.31(7)
N(8)–Mn(1)–N(11)	86.07(8)	86.17(7)
N(8)–Mn(1)–N(10A)	90.2(1)	89.33(8)
N(8)–Mn(1)–N(13B)	94.24(9)	95.31(8)
N(11)–Mn(1)–N(10A)	92.64(9)	92.51(7)
N(11)–Mn(1)–N(13B)	177.58(9)	176.69(7)
N(10A)–Mn(1)–N(13B)	89.77(9)	90.47(7)

Symmetry transformations used to generate equivalent atoms: A: $-x+1, -y+2, -z$; B: $x-1, y, z$.

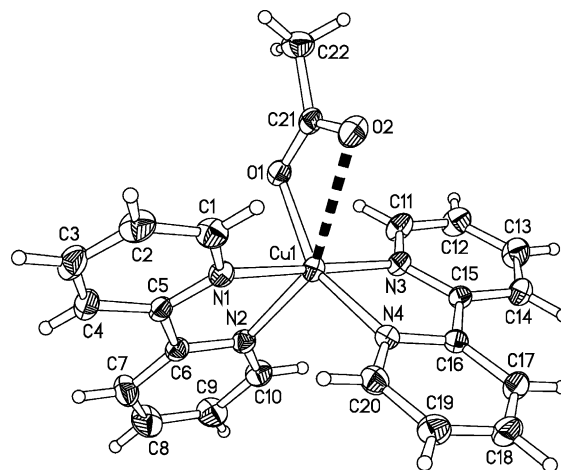


Fig. 1. ORTEP and atom labelling diagram for the $[Cu(OAc)(bpy)_2]^+$ cation in $[Cu(OAc)(bpy)_2][Mn(dca)_3(H_2O)]$ (**1**). The long Cu1–O2 bond is shown by a dashed solid bond.

on a Nonius KappaCCD diffractometer with graphite-monochromated Mo $K\alpha$ radiation ($\lambda = 0.71073$ Å) [12]. Cell parameters were obtained by the global refinement of the positions of all reflections [13], and an empirical absorption was applied [14,15]. Both structures were solved by direct methods and refined by full-matrix least-squares on F^2 [16]. All non-H atoms were refined anisotropically. The H atoms attached to C atoms were added at calculated positions and not refined. The H atoms of the aqua ligand were located from the difference Fourier synthesis and refined using constrained geometry of the free water molecule.

3. Results and discussion

3.1. Description of the structures

Selected bond distances and bond angles for complexes **1** and **2** are given in Table 2. Complexes **1** and **2** are isomorphous, so the structure of **1**, the Cu complex, is discussed here in detail.

The positively charged building block in **1** is the $[Cu(OAc)(bpy)_2]^+$ cation (Fig. 1), in which the Cu^{2+} ion is chelated by two bpy and one OAc anion, in a distorted octahedral environment. Its geometry is similar to that of the cation found in, for instance, $[Cu(OAc)(bpy)_2][Cu(bpy)_2(Cr(C_2O_4)_3)] \cdot 10.5H_2O$ [17]. In the lattice, two cations first form a dimer (Fig. 2) through a pair of weak C–H \cdots O hydrogen bonds [18] ($C17-H13 \cdots O2$: H \cdots O 2.55 Å, C \cdots O 3.241 Å, and angle C–H \cdots O 131.2°) and the π – π interaction between two face-to-face bpy ligands with a separation of 3.55 Å between their mean planes. The dimers further form a layer through another weak π – π interaction (face-to-face distance: 3.84 Å) between the bpy ligands and the C–H \cdots π interaction [18] between the methyl group

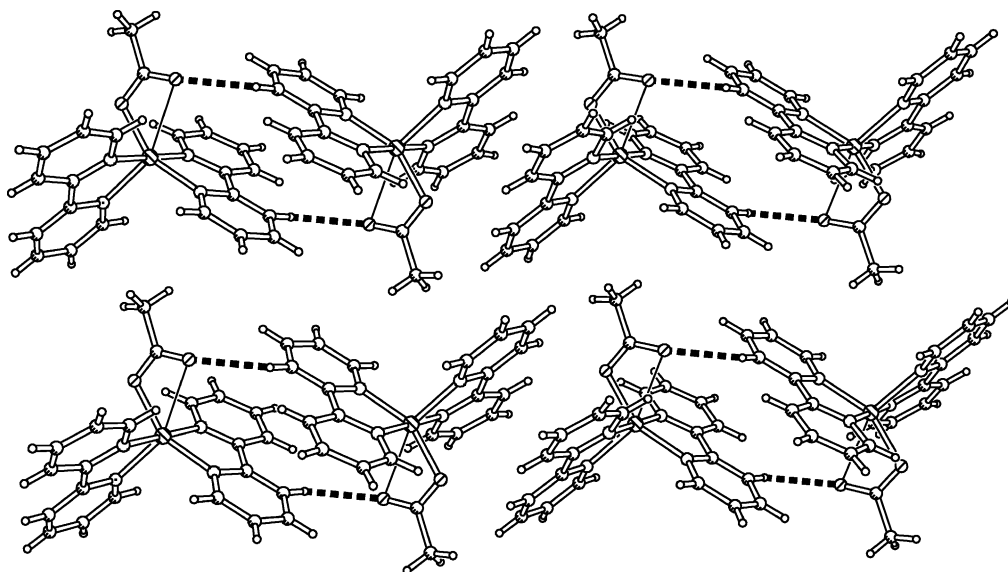


Fig. 2. Cationic layer made up of $[\text{Cu}(\text{OAc})(\text{bpy})_2]^+$ cations in **1** showing the weak $\text{C}-\text{H}\cdots\text{O}$ hydrogen bond (dotted lines), $\pi-\pi$ interaction and $\text{C}-\text{H}\cdots\pi$ interaction.

(C22) of OAc and its neighbouring pyridyl ring (C6 to C10 and N2) at a distance of 3.647 Å from C22 to the centroid of the pyridyl ring.

The negatively charged building parts of the structure is the ladder-like chain $[\text{Mn}(\text{dca})_3(\text{H}_2\text{O})^-]_n$ (Fig. 3). In the chain, two Mn^{2+} ions are first linked by two $\mu_{1,5}$ -dca's to form a dimer. Together with the two dca's, one aqua ligand and one terminal dca occupy the four

equatorial sites around each Mn^{2+} ion. Then in the axial direction, the neighbouring dimers are connected by another two $\mu_{1,5}$ -dca's to build a ladder chain running along the a axis, with the dimers as the rungs of the ladder. Meanwhile, this linkage completes the octahedral configuration for each Mn^{2+} ion. The grids in the ladder are 7.321 Å wide and 8.859 Å long. The ladder is different from another type of ladder,

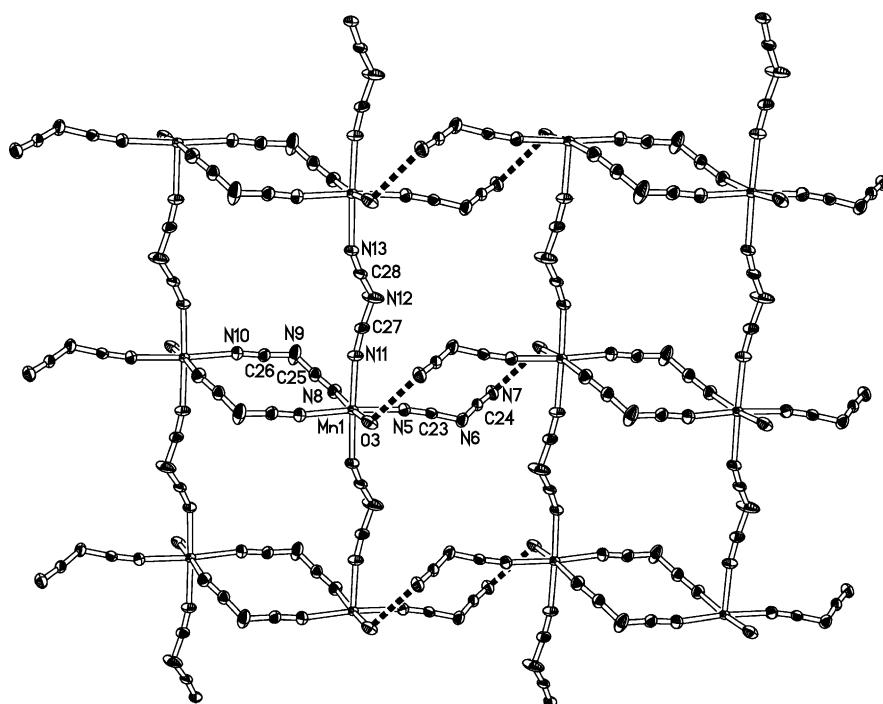


Fig. 3. Pseudo-(4,4) sheet composed of $[\text{Mn}(\text{dca})_3(\text{H}_2\text{O})^-]_n$ ladder chains through hydrogen bonds (dotted lines) in **1**, with atomic labelling scheme.

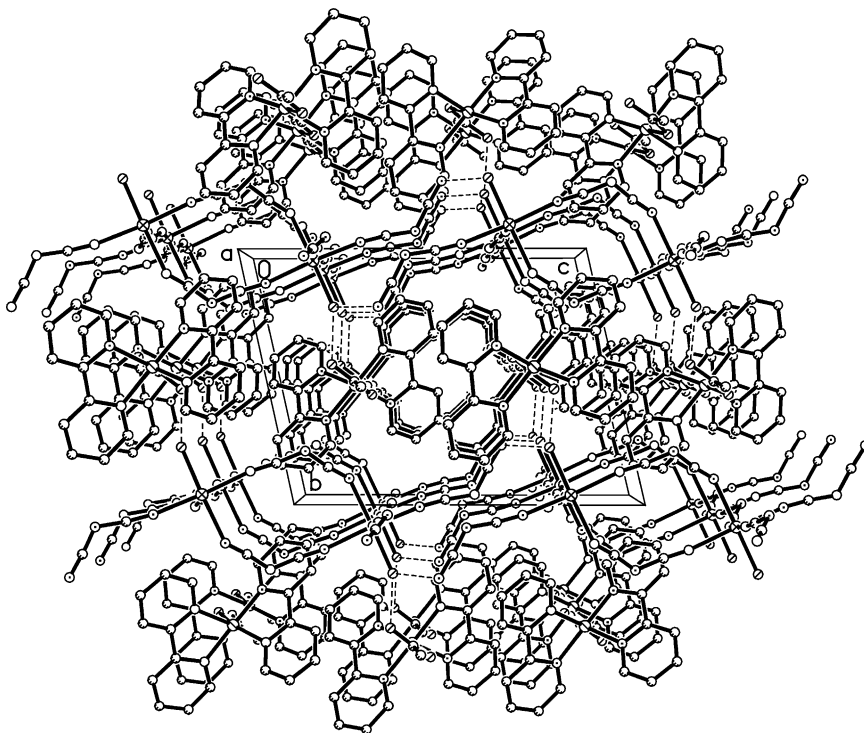


Fig. 4. Sandwich crystal structure of **1** viewed down the *a* axis. Dashed lines show the N...O and O...O hydrogen bonds.

$[\text{M}_2(\text{dca})_6(\text{H}_2\text{O})]^{2-}$ ($\text{M} = \text{Co}$ or Ni) previously reported [10c], but similar to that in $\text{Mn}[\text{N}(\text{CN})_2]_2(\text{H}_2\text{O})(\text{NH}_2\text{-pyz})_{1.5}$ [2g]. These ladder chains arrange in the *ac* plane and form a pseudo- (4,4) negative-charged net via hydrogen bonds between the aqua ligand of one chain and the free terminal N atoms of the non-bridging dca ligands of the neighbouring chains, with N...O distances of 2.813 Å. In the 2-D net the other type of grid size is 8.636×8.859 Å.

The cationic and anionic sheets stack along the *b* axis alternately (Fig. 4), thus forming a bimetallic sandwich structure. In the crystal structure, the OAc group of the cation points to the aqua ligand of a neighbouring Mn^{2+} ion, and thus another strong hydrogen bond is formed with an O...O distance of 2.699 Å. The ability of the $[\text{Cu}(\text{OAc})(\text{bpy})_2]^+$ cation to form hydrogen bonds is the main feature that distinguishes this template cation from other arylated cations [8,10], which are usually involved only in concerted C-H... π and π - π interactions. There are also a number of weak interactions with H...C/N/O distances of 2.781–2.976 Å between the cationic and the anionic sheets.

No significant structural difference exists between **1** and **2**, except that the long Cu1–O2 bond of 2.672 Å in **1** becomes the shorter Zn1–O2 of 2.347 Å in **2**.

3.2. EPR spectra

At room temperature, the EPR spectra, recorded on the polycrystalline samples of the two compounds, show

a strong isotropic Lorentzian signal at $g = 2.00$. The peak-to-peak line widths, ΔH_{pp} , are 160 and 130 G for **1** and **2**, respectively. A weak half-field signal at $g = 4.00$ was observed for both of them. These broad signals indicate that there are super-exchange interactions among spin centers [3b].

3.3. Magnetic properties

The $\chi_{\text{M}}T$ product versus T in the 300–2 K range for **1** and **2** is plotted in Fig. 5, in a field of 10 kOe. The values of $\chi_{\text{M}}T$ at room temperature are 4.73 and 4.36 $\text{cm}^3 \text{mol}^{-1} \text{K}$, for **1** and **2**, respectively. They are in well agreement with the spin-only value expected for an uncoupled $\text{Cu}^{\text{II}}\text{Mn}^{\text{II}}$ (4.75 $\text{cm}^3 \text{mol}^{-1} \text{K}$) or Mn^{II} (4.37 $\text{cm}^3 \text{mol}^{-1} \text{K}$) system. In each compound, the $\chi_{\text{M}}T$ value remains nearly constant to about 50 K then decreases rapidly toward 2.11 and 1.67 $\text{cm}^3 \text{mol}^{-1} \text{K}$ at 2 K. Both compounds show the Curie–Weiss behaviour in the whole temperature region of measurement. The Weiss constants, θ 's, obtained by fitting the data to the Curie–Weiss expression, $\chi = C(T - \theta)^{-1}$, are $-2.78(2)$ ($R = 8.4 \times 10^{-5}$) and $-3.62(3)$ K ($R = 2.8 \times 10^{-4}$) for **1** and **2**, respectively (R is defined as $R = \Sigma[(\chi_{\text{M}})_o - (\chi_{\text{M}})_c]^2 / \Sigma[(\chi_{\text{M}})_o]^2$).

As is generally known, it is difficult to estimate the exchange interaction within Mn^{2+} ladder complexes. In this work, we adopt a simple model to explain the magnetic behaviour of these compounds. First, we consider the magnetic susceptibility of the dimer [19]

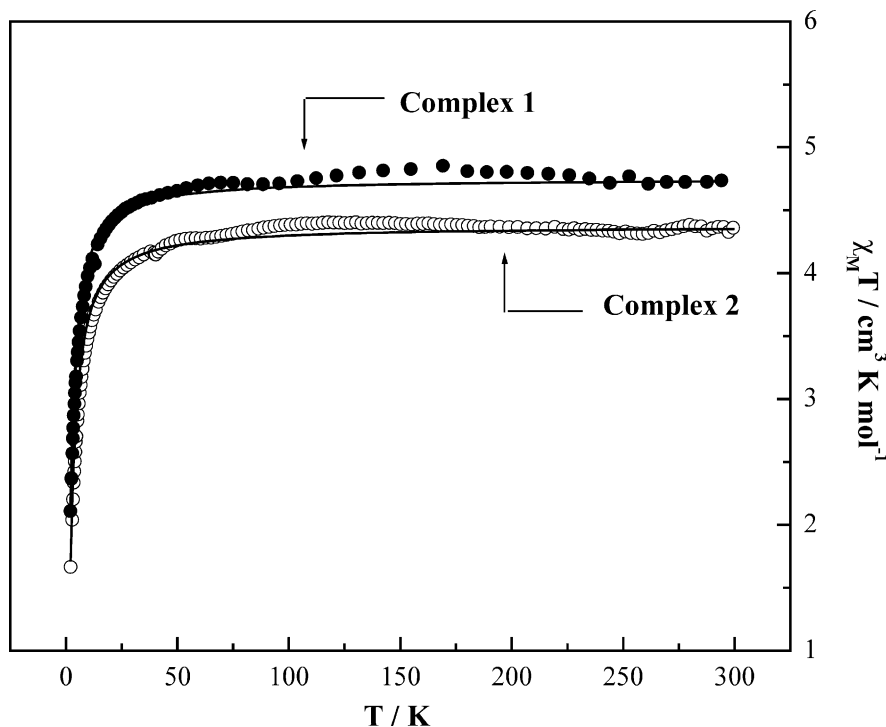


Fig. 5. Temperature dependence of the $\chi_M T$ product of $[\text{Cu}(\text{OAc})(\text{bpy})_2][\text{Mn}(\text{dca})_3(\text{H}_2\text{O})]$ (**1**) and $[\text{Zn}(\text{OAc})(\text{bpy})_2][\text{Mn}(\text{dca})_3(\text{H}_2\text{O})]$ (**2**). The dots are experimental values, the solid lines represent the best calculated curves (see text).

in the Mn–dca ladder

$$\chi_d = \frac{Ng^2\beta^2}{3k_B T} \frac{(55 + 30e^{10x} + 14e^{18x} + 5e^{24x} + e^{28x})}{(11 + 9e^{10x} + 7e^{18x} + 5e^{24x} + 3e^{28x} + e^{30x})}$$

$$x = -J_1/k_B T$$

where J_1 is the intra-dimer coupling constant, N the Avogadro's number, β the Bohr magneton, and k the Boltzmann's constant. The dimeric unit is assumed to act as an effective S_d classical spin system [20] with

$$S_d = [-1 + [1 + 4(\chi_d T / (0.125 \text{g}^2))]^{1/2}] / 2$$

Then, the ladder chain can be treated as the linkage of dimers and its contribution, χ_{chain} , to the total magnetic susceptibility χ , according to the Fisher's model [21] is

$$\chi_{\text{chain}} = \frac{Ng^2\beta^2 S_d(S_d + 1)}{3k_B T} \frac{1 + u}{1 + u}$$

$$u = \coth \left[\frac{2J_2 S_d(S_d + 1)}{k_B T} \right] - \frac{kT}{2J_2 S_d(S_d + 1)}$$

where J_2 is the inter-dimer coupling constant.

The Cu complex cations in **1** can be treated as paramagnetic parts, as each is surrounded by ligands and has no linkage with Mn^{2+} or another Cu^{2+} ion. So the contribution of the cations, χ_{Cu} , is

$$\chi_{\text{Cu}} = \frac{Ng^2\beta^2 S_{\text{Cu}}(S_{\text{Cu}} + 1)}{3k_B T}$$

Thus, the total magnetic susceptibility $\chi = \chi_{\text{chain}} + \chi_{\text{Cu}}$. In **2**, the Zn complex cation makes no contribution.

The parameters corresponding to the best fit for J_1 and J_2 are -0.17 and -0.01 cm^{-1} for **1**, and -0.18 and -0.02 cm^{-1} for **2**, which are similar to those found in other Mn–N≡C–N–C≡N–Mn compounds [3b,3c]. The very small values of J indicate that weak antiferromagnetic intrachain interactions are mediated by the $\mu_{1,5}$ -dca pathway [3c].

4. Conclusion

Two isomorphous bimetallic polymers were synthesized utilizing Cu- or Zn-bpy-acetate cations and Mn–dca polymer anions. In addition to containing a unique structural feature, namely, heterometallic sandwich of cationic complex layers and anionic sheets of ladders, the compounds provided the opportunity to study the magnetic inter-exchange effect in a ladder system. As the $\mu_{1,5}$ -dicyanamide bridge is a very poor super-exchange mediator [3c], only very weak antiferromagnetic coupling between Mn–Mn centers are observed for these compounds.

5. Supplementary material

Crystallographic data (excluding structure factors) for the structures reported in this paper have been deposited

with the Cambridge Crystallographic Data Centre, CCDC Nos. 162534 and 162535 for complexes **1** and **2**. Copies of this information may be obtained free of charge from The Director, CCDC, 12 Union Road, Cambridge, CB2 1EZ, UK (fax: +44-1223-336033; e-mail: deposit@ccdc.cam.ac.uk or www: <http://www.ccdc.cam.ac.uk>).

Acknowledgements

The authors gratefully thank the financial support of the NSFC (Nos. 90201014 & 29831010), the MOST of China (No. G1998061310) and the Founder Foundation of Peking University.

References

- [1] J.S. Miller, J.L. Manson, *Acc. Chem. Res.* 34 (2001) 563 (and references cited in).
- [2] For the most recent reports, see (a) B. Vangdal, J. Carranza, F. Lloret, M. Julve, J. Sletten, *J. Chem. Soc., Dalton Trans.* (2002) 566; (b) J.L. Masson, C.R. Kmety, F. Palacio, A.J. Epstein, J.S. Miller, *Chem. Mater.* 13 (2001) 1068; (c) J.L. Manson, Q. Huang, J.W. Lynn, H.-J. Koo, M.-H. Whangbo, R. Bateman, T. Otsuka, N. Wada, D.N. Argyriou, J.S. Miller, *J. Am. Chem. Soc.* 123 (2001) 162; (d) P. Jensen, S.R. Batten, B. Moubaraki, K.S. Murray, *J. Solid State Chem.* 159 (2001) 352; (e) S. Martin, M.G. Barandika, J.I.R. de Larramendi, R. Cortes, M. Font-Bardia, L. Lezama, Z.E. Serna, X. Solans, T. Rojo, *Inorg. Chem.* 40 (2001) 3687; (f) S. Triki, F. Thetiot, J.-R. Galan-Mascaros, J.S. Pala, K.R. Dunbar, *New J. Chem.* 25 (2001) 954; (g) J.L. Manson, J.A. Schlueter, U. Geiser, M.B. Stone, D.H. Reich, *Polyhedron*, 20 (2001) 1423.
- [3] (a) S. Martin, M.G. Barandika, R. Cortes, L. Ruiz, M.K. Urriaga, L. Lezama, M.I. Arriortua, T. Rojo, *Eur. J. Inorg. Chem.* 8 (2001) 2107; (b) A. Escuer, F.A. Mautner, N. Sanz, R. Vicente, *Inorg. Chem.* 39 (2000) 1668; (c) J.L. Manson, A.M. Arif, C.D. Incarvito, L.M. Liable-Sands, A.L. Rheingold, J.S. Miller, *J. Solid State Chem.* 145 (1999) 369.
- [4] (a) S.R. Batten, P. Jensen, B. Moubaraki, K.S. Murray, R. Robson, *Chem. Commun.* (1998) 439; (b) M. Kurmoo, C.J. Kepert, *New J. Chem.* (1998) 1515; (c) J.L. Manson, C.R. Kmety, Q. Huang, J.W. Lynn, G.M. Bendele, S. Pagola, P.W. Stephen, L.M. Liable-Sands, A.L. Rheingold, A.J. Epstein, J.S. Miller, *Chem. Mater.* 10 (1998) 2552.
- [5] (a) S.R. Batten, P. Jensen, C.J. Kepert, M. Kurmoo, B. Moubaraki, K.S. Murray, D.J. Price, *Chem. Commun.* (1999) 177; (b) J.L. Manson, D.W. Lee, A.L. Rheingold, J.S. Miller, *Inorg. Chem.* 37 (1998) 5966.
- [6] B.W. Sun, S. Gao, Z.M. Wang, *Chem. Lett.* (2001) 2.
- [7] S.R. Batten, P. Jensen, B. Moubaraki, K.S. Murray, *Chem. Commun.* (2000) 2331.
- [8] Z.M. Wang, B.W. Sun, J. Luo, S. Gao, C.S. Liao, C.H. Yan, *Inorg. Chim. Acta* 332 (2002) 127.
- [9] Z.M. Wang, B.W. Sun, J. Luo, S. Gao, C.S. Liao, C.H. Yan, to be submitted.
- [10] (a) J.W. Raebiger, J.L. Manson, R.D. Sommer, U. Geiser, A.L. Rheingold, J.S. Miller, *Inorg. Chem.* 40 (2001) 2578; (b) P.M. van der Werff, S.R. Batten, P. Jensen, B. Moubaraki, K.S. Murray, *Inorg. Chem.* 40 (2001) 1718; (c) P.M. van der Werff, S.R. Batten, P. Jensen, B. Moubaraki, K.S. Murray, E.H.-K. Tan, *Polyhedron* 20 (2001) 1129.
- [11] O. Kahn, *Molecular Magnetism*, VCH, New York, 1993.
- [12] 'Collect' data collection software, Nonius B.V., Delft, The Netherlands, 1998.
- [13] Z. Otwinowski, W. Minor, *Methods Enzymol.* 276 (1997) 307.
- [14] (a) R.H. Blessing, *Acta Crystallgr., Sect. A* 51 (1995) 33; (b) R.H. Blessing, *J. Appl. Cryst.* 30 (1997) 421.
- [15] S. Mackay, C.J. Gilmore, C. Edwards, M. Tremayne, N. Stuart, K. Shankland, 'maXus: a computer program for the solution and refinement of crystal structures from diffraction data', University of Glasgow, Scotland, UK, Nonius BV, Delft, The Netherlands and MacScience Co. Ltd., Yokohama, Japan, 1998.
- [16] (a) G.M. Sheldrick, *SHELXTL Version 5.10*. Bruker Analytical X-ray, Instruments Inc., Madison, WI, USA, 1998.; (b) G.M. Sheldrick, *SHELX-97, PC Version*, University of Göttingen, Germany, 1997.
- [17] O. Costisor, K. Mereiter, M. Julve, F. Lloret, Y. Journaux, W. Linert, M. Andruh, *Inorg. Chim. Acta* 324 (2001) 352.
- [18] G.R. Desiraju, T. Steiner, *The Weak Hydrogen Bond in Structural Chemistry and Biology*, Oxford University Press, New York, 1999.
- [19] R. Cortes, M.K. Urriaga, L. Lezama, J.L. Pizarro, M.I. Arriortua, T. Rojo, *Inorg. Chem.* 36 (1997) 5016.
- [20] B. Chiari, A. Cinti, L. David, F. Ferraro, D. Gatteschi, O. Piovesana, P.F. Zanazzi, *Inorg. Chem.* 35 (1996) 7413.
- [21] (a) M.E. Fisher, *Am. J. Phys.* 32 (1964) 343; (b) T. Smith, S.A. Friedberg, *Phys. Rev.* 176 (1968) 660.